ORIGINAL PAPER

CrossMark

Brain Network Reconfiguration During Motor Imagery Revealed by a Large-Scale Network Analysis of Scalp EEG

Fali Li[1] · Chanlin Yi[1] · Limeng Song[1] · Yuanling Jiang[1] · Wenjing Peng[1] · Yajing Si[1] · Tao Zhang[1] · Rui Zhang[2] · Dezhong Yao[1,3] · Yangsong Zhang[1,4] · Peng Xu[1,3]

Abstract
Mentally imagining rather physically executing the motor behaviors is defined as motor imagery (MI). During MI, the mu rhythmical oscillation of cortical neurons is the event-related desynchronization (ERD) subserving the physiological basis of MI-based brain-computer interface. In our work, we investigated the specific brain network reconfiguration from rest idle to MI task states, and also probed the underlying relationship between the brain network reconfiguration and MI related ERD. Findings revealed that comparing to rest state, the MI showed the enhanced motor area related linkages and the deactivated activity of default mode network. In addition, the reconfigured network index was closely related to the ERDs, i.e., the higher the reconfigured network index was, the more obvious the ERDs were. These findings consistently implied that the reconfiguration from rest to task states underlaid the reallocation of related brain resources, and the efficient brain reconfiguration corresponded to a better MI performance, which provided the new insights into understanding the mechanism of MI as well as the potential biomarker to evaluate the rehabilitation quality for those patients with deficits of motor function.

Introduction

Motor imagery (MI) refers to the mental imagery of the required motor tasks without the physical motor output (Lotze and Halsband 2006; Sharma and Baron 2013), and it has been widely used in motor skills learning, neurological rehabilitation, and brain-computer interface (BCI) (Blankertz et al. 2010; Burianová et al. 2013; Long et al. 2012; Miller et al. 2010; Mulder 2007). The MI-based BCI (MI-BCI) is usually used to extend the healthy individual's ability (Li et al. 2010; Yu et al. 2012), to provide the compensative assistance to disabled patients (Li et al. 2016b, 2013), and to avail the rehabilitation of motor function (Mulder 2007; Sharma et al. 2006). During MI, the power decrease at mu rhythm occurs prominently over the contralateral sensorimotor area, which is defined as the event-related desynchronization (ERD) (Friedrich et al. 2009; Pfurtscheller and Da Silva 1999) subserving the useful feature corresponding to the movement volition (Pfurtscheller and Neuper 1997).

Multiple neuroimaging technologies including functional magnetic resonance imaging (fMRI) and electroencephalography (EEG) are usually considered to capture the brain activity during MI. However, benefiting from its high temporal resolution, low cost, and easy operation, EEG is frequently adopted to probe the neural mechanism of MI (Li et al. 2018; Toppi et al. 2015; Zhang et al. 2015). In essence, the brain functions as a complex network, the information is processed between those specialized, spatially distributed but functionally linked regions (Bullmore

and Sporns 2009; Iturria-Medina et al. 2008; Sharma and Baron 2013; Sporns et al. 2000; Stam and Van Straaten 2012). The brain network analysis can be used to probe the underlying neural mechanism, and based on those brain networks, the measured inter-regional linkages can mark out the corresponding dynamic information processing patterns (Friston et al. 2003; Li et al. 2016a; Toppi et al. 2015). In real applications, either anatomical tract, or functional connectivity measured by coherence, phase locking value, and etc. is usually considered to construct the brain networks (Li et al. 2015; Sakkalis 2011; Zhang et al. 2015).

Our brain is not idle, even at rest (Raichle et al. 2001); the spontaneous activity may reflect the brain's potential ability to efficiently process the related information during tasks (Ramos-Loyo et al. 2004; van den Heuvel and Hulshoff Pol 2010; Zhang et al. 2016). Resting-state fMRI study shows that human intellectual performance is dependent on the efficiency of brain in integrating information across distributed regions (van den Heuvel et al. 2009); studies based on clinical diseases (i.e., epilepsy) prove the possibility of resting-state network in understanding the underlying pathophysiological mechanisms (Xu et al. 2014a, b; Yao et al. 2010; Zhang et al. 2011); and our previous study also demonstrates that the efficient brain at rest facilitates the subjects' BCI performance (Zhang et al. 2015). Apart from the resting-state studies, the task-related MIs have been further investigated (Burianová et al. 2013; Pilgramm et al. 2016), as well. Brain regions including premotor cortex (PMc), parietal areas, and supplemental motor area (SMA) are proved to be activated and involved in the information processing of MI (Miller et al. 2010; Sharma and Baron 2013).

Even previous studies have probed the underlying mechanism that accounts for the variability of MI across individuals, based on either rest- or task-related studies, few of related studies have considered the relationship between the brain activity under these two types of states, meanwhile how the brain reorganizes from rest idle state to fulfill the needs of MI is still left unveiled. In fact, the brain at rest determines the degree of how brain can be reconfigured in following tasks, and the network update efficiency correlated with the individuals' general intelligence (Schultz and Cole 2016). Exploring how large-scale functional networks are reconfigured between task and rest can facilitate clarifying how the human brain responds to a specific task at the network level. Therefore, in this study, we assume that the brain reconfiguration from rest to task states may play important roles in the information processing during MI, based on which we endeavor to probe how the brain reorganizes from rest idle to MI task states and also probe the relationship between the brain reorganization and the MI.

Experimental Procedures

Participants

The experiment was approved by the Institution Research Ethics Board of the Key Laboratory of NeuroInformation of Ministry of Education at University of Electronic Science and Technology of China and conformed to the principles of the Declaration of Helsinki. Before the experiment, all participants were asked to read and sign an informed consent form. 26 healthy postgraduates (9 females, aged 22.23 ± 4.23 years, 2 left-handed) were paid for their time and effort to participate in our experiment. All participants had the normal or correct-to-normal vision. None of them had the habitual drug, alcohol consumption, cognitive impairments, and neurological disorders.

MI Experiments

The current MI experiment consisted of a 2-min eye-closed resting-state and the following left- or right-hand MIs. Between two adjacent experimental stages, a 2-min break was given to all subjects. And 4 runs of MIs were then performed as the subjects were informed to perform the imagery of bouncing a ball by his/her left or right hand according to the instructions presented on the computer screen (Fig. 1). For each MI run, a total of 50 trials with 25 trials for left-hand MIs (lMIs) and 25 trials for right-hand MIs (rMIs) were included. For each MI trial, the task would start with a 4-s rest; after that, 1-s yellow bar appeared on the left or right side of the screen to remind the subjects to fully prepare to perform the MI task; and after the bar turned green, the subjects were given 5 s to perform the required MI task.

Data Acquisition

Using the Symtop amplifier (Symtop Instrument, Beijing, China), the rest and task EEG datasets with 15 Ag/AgCl electrodes from extended international 10–20 system were recorded. During online recording, the EEGs were band-pass filtered with frequency band of 0.5–45 Hz, sampled with sampling rate of 1000 Hz. Electrode AFz served as the reference. And across the whole experiments, the impedance for each electrode was kept below 10 kΩ.

Data Analysis

In the present study, aiming to probe the underlying relationships between brain reconfiguration from rest to task states and subjects' task performance (i.e., ERDs), we implemented a series of processes based on the recorded scalp

Fig. 1 EEG experimental paradigm with the rest and task datasets recording. Each MI trial consisted of the following periods: a 4-s rest period, represented by the gray bars presented at the both sides of computer screen; a 1-s cue, represented by the yellow bar presented at the left/right side of computer screen; and a 5-s motor imagery task, represented by the green bar presented at the left/right side of computer screen
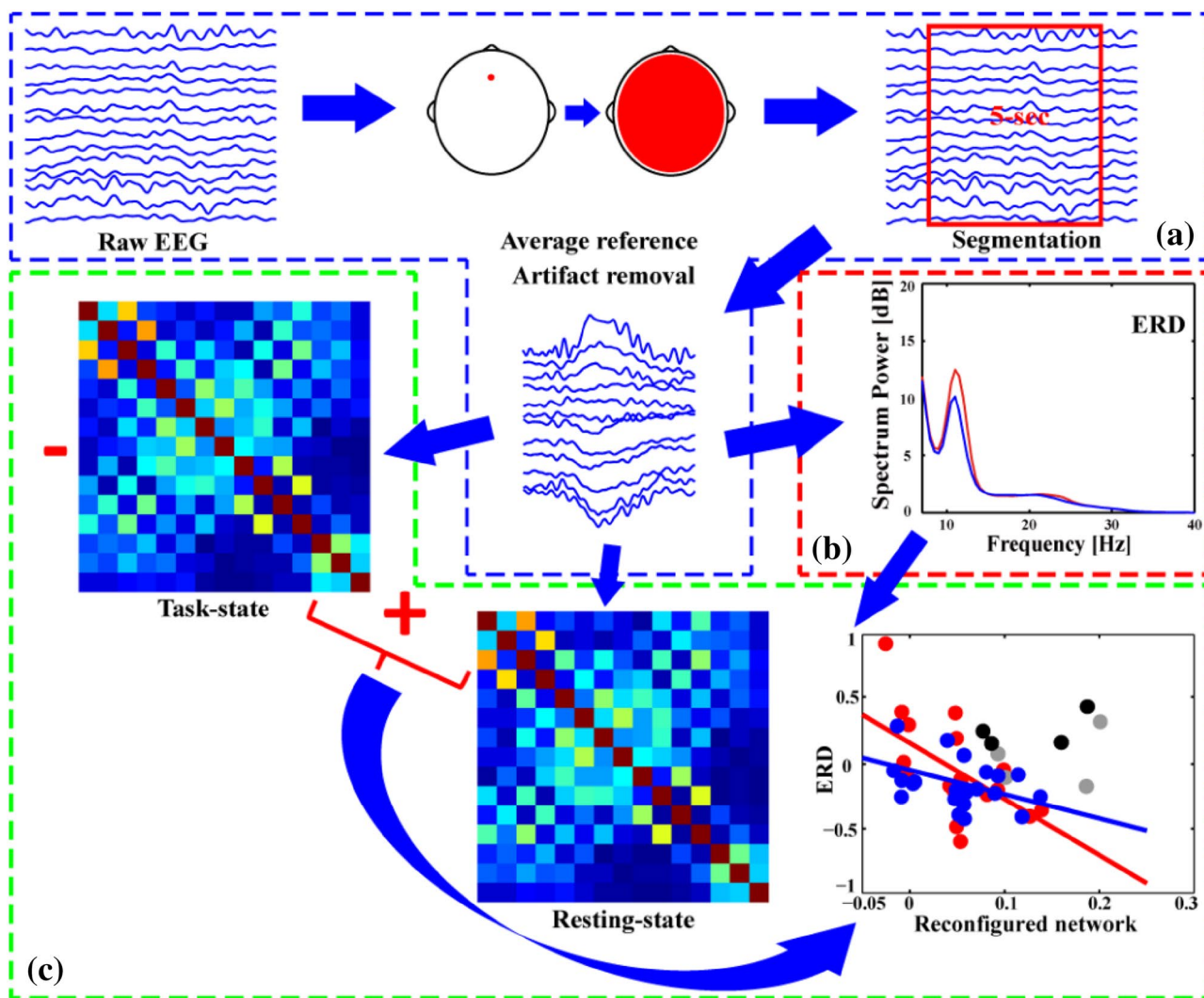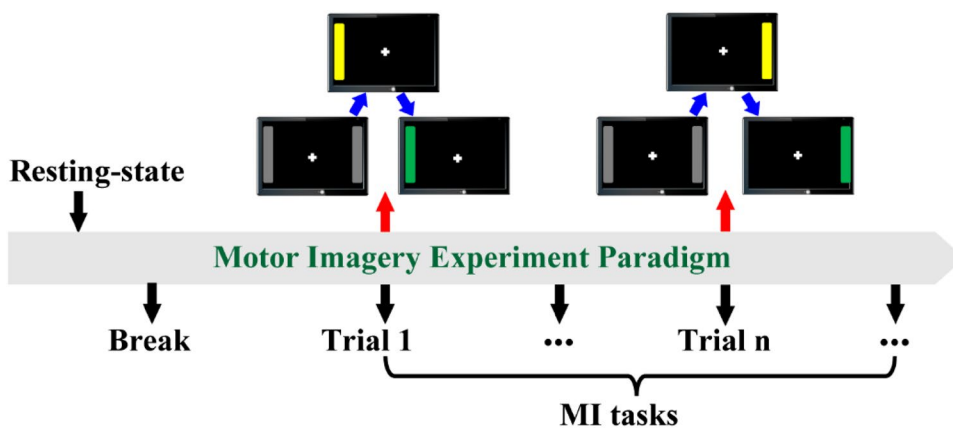

Fig. 2 The processing procedures for the rest and task EEG datasets. **a** EEGs pre-processing, **b** ERD calculation, **c** ERD versus reconfigured network

EEGs, which included the data pre-processing, ERD calculation, and correlation analysis between ERD and brain reconfiguration parameters (Fig. 2). And the details for each process were further provided in following portions.

Data Pre-processing

Before network construction, the multiple pre-processing procedures were considered to exclude the contained artifacts, and the related procedures consisted of averaging re-referencing, 0.5–30 Hz offline band-pass filtering, data segmentation, and artifacts removal (± 75 uv as threshold). Since resting-state EEGs showed the spontaneous brain activity during the idle state, while the MI task EEGs recorded the event-related activity during required task, in the procedure of data segmentation, the distinct processes were performed to divide the whole length of EEGs into numbers of artifact-free data segments. Meanwhile, since the designed MI task consisted of 4-s rest, 1-s cue, and 5-s task periods and the subjects only perform the MI task during the related 5-s task period, to promise the consistency of data analysis between rest and task states, the 5-s window is also applied to the resting-state EEG to divide it into segments for the further analysis.

Resting-State EEG For resting-state EEGs, during the process of data segmentation, the first and last 10 s of EEGs were excluded, while the remaining data was divided into numbers of 5-s segments. Afterwards, the coherence was adopted to construct the corresponding networks (i.e., adjacency matrix) for each 5-s segment. And finally, the adjacency matrix was averaged across all segments to estimate the individual resting-state connectivity matrix for each subject.

MI Task EEG For MI task EEGs, relying on the time point recorded (i.e., the onset of bar turning green) where the subjects started to perform the required lMIs or rMIs, the following 5-s length of EEGs for each MI trial were extracted. And after that, the similar procedure of network construction was also adopted to estimate the connectivity matrix for each MI trial, meanwhile based on which the average was performed to achieve the individual's connectivity matrix of lMIs or rMIs.

Brain Network Analysis

After pre-processing, all of the artifact-free rest/task trials were used to construct the rest/task brain networks for each subject. The same coherence analysis (Zhang et al. 2015) was adopted in current study to measure the linkages between each pair of electrodes. Specifically, considering $x(t)$ and $y(t)$ in each MI trial, coherence is defined as

$$C_{xy}(f) = \frac{\left|P_{xy}(f)\right|}{P_{xx}(f)P_{yy}(f)} \tag{1}$$

where $P_{xy}(f)$ is the cross-spectral density between $x(t)$ and $y(t)$ at the frequency f, $P_{xx}(f)$ and $P_{yy}(f)$ are the auto-spectral densities of $x(t)$ and $y(t)$ at the frequency f, respectively, and $C_{xy}(f)$ is the frequency-dependent coherence. Then, the edge linkages were estimated by averaging the coherence value within the concerned frequency band, which led to the 15×15 weighted adjacency matrix for each artifact-free segment. For each subject, the final weighted network was obtained by averaging the connectivity matrices of those artifact-free segments.

Let w_{ij} and d_{ij} represent the coherence value and shortest path length between nodes i and j, respectively, n represent the node number, and Ψ represent the set of nodes. For each subject, the local electrode and global network parameters were then calculated by adopting the brain connectivity toolbox (BCT, http://www.nitrc.org/projects/bct/) (Rubinov and Sporns 2010).

Clustering coefficient (*CC*) and local efficiency (*LE*) both relate to the estimation of the potential for functional segregation between brain areas, and consistently reflect the potential capacity of local information processing in the brain. The related *CC* and *LE* on each electrode (*eCC* and *eLE*) can be formulated as,

$$eCC_i = \frac{\sum\limits_{j,h\in\Psi} \left(w_{ij}w_{ih}w_{jh}\right)^{1/3}}{\sum\limits_{j\in\Psi} w_{ij}\left(\sum\limits_{j\in\Psi} w_{ij} - 1\right)} \tag{2}$$

$$eLE_i = \frac{\sum\limits_{j,h\in\Psi,j\neq i} \left(w_{ij}w_{ih}\left[d_{jh}(\Psi_i)\right]^{-1}\right)^{1/3}}{\sum\limits_{j\in\Psi} w_{ij}\left(\sum\limits_{j\in\Psi} w_{ij} - 1\right)} \tag{3}$$

On the contrary, characteristic path length (*CPL*) and global efficiency (*GE*) estimate the potential for functional integration between brain regions, and consistently represent the brain efficiency of global information processing, therefore they can be calculated as follows,

$$CPL = \frac{1}{n}\sum\limits_{i\in\Psi}\frac{\sum\limits_{j\in\Psi,j\neq i} d_{ij}}{n-1} \tag{4}$$

$$GE = \frac{1}{n}\sum\limits_{i\in\Psi}\frac{\sum\limits_{j\in\Psi,j\neq i}\left(d_{ij}\right)^{-1}}{n-1} \tag{5}$$

Meanwhile, by averaging the calculated *eCC* and *eLE* across all concerned fifteen electrodes, the *CC* and *LE* are further calculated as,

$$CC = \frac{\sum_{i \in \Psi} eCC_i}{n} \tag{6}$$

$$LE = \frac{\sum_{i \in \Psi} eLE_i}{n} \tag{7}$$

Cortical Activity Measure: ERD

As illustrated, over the contralateral sensorimotor area, the related power decrease could be clearly found at specific rhythm (i.e., mu rhythm) when the subjects were required to perform the lMIs and rMIs (Friedrich et al. 2009; Pfurtscheller and Da Silva 1999; Pfurtscheller and Neuper 1997). In the current study, for either lMIs or rMIs, the corresponding power spectrums on electrodes C3 and C4 were firstly statistically compared by using paired *t*-test, and the related ERDs were then calculated for lMIs or rMIs of each subject.

In fact, ERD is a useful biomarker to explore the brain sensory, motor, and cognitive function under both the normal and pathological conditions, which has been widely used to measure the capacity of subjects' MI ability (Graimann et al. 2002; Lotze and Halsband 2006). In our present study, the corresponding ERDs (i.e., C3-ERD for rMIs and C4-ERD for lMIs) were formulated as,

$$\chi = \frac{\beta(task) - \beta(rest)}{\beta(rest)} \tag{8}$$

where χ denotes the ERDs of electrodes C3 for rMIs and C4 for lMIs, and $\beta(\cdot)$ denotes the sum of power spectrum at mu rhythm of rest or task state.

Reconfigured Network Index

In our present study, aiming to probe the possible relationships between the reconfigured brain networks from rest to task and the MI related ERDs, based on the properties of rest and task networks, the new network parameter, reconfigured network index (rCNI), defined as the subtraction of properties between rest and task networks was proposed to quantitatively measure the change of brain efficiency in task from that at rest, which was formulated in Eq. (9) as,

$$\delta' = \delta(rest) - \delta(task) \tag{9}$$

where δ' represents the reconfigured network index and $\delta(\cdot)$ represents the properties of rest/task network.

Correlation Analysis

In this work, to probe how the brain reconfigures from rest idle state to meet the needs of MI and to uncover the relationships between MI related ERDs and reconfigured brain networks, we firstly measured the reorganized brain network topologies from rest to lMIs/rMIs by using the paired *t*-test and corrected by using false discovery rate (FDR). Then, based on the measured global network and local electrode parameters, the differences of related network parameters between two distinct states were also measured by paired *t*-test. Afterwards, the relationships of rest vs. task networks and ERD vs. reconfigured network were finally analyzed by Person's Correlation analysis. Specially, in this work, we used the proposed rCNI to quantitatively evaluate the brain reconfiguration from rest to task states with its role in facilitating the information processing of MI.

Outlier Subjects Removing Strategy

When conducting correlation analysis between rCNI and ERDs, some obvious outliers that deviate from the data center would weaken the underlying relations. In the present study, in order to obtain the robust representative knowledge that accounts for the brain reconfiguration from rest to task states, the outliers were selected based on an analysis of relationships between rCNI and ERDs. Afterwards, the subjects with the 10% largest Malahanobis distances (Zhang et al. 2015) to the data center were considered as the outliers, and further excluded from analysis of relationships between rCNI and ERDs.

Results

Reconfigured Networks in MI

Figure 3 reveals the reorganized network topologies from rest idle to lMIs/rMIs ($p < 0.05$, paired *t*-test, FDR correction). As revealed in Fig. 3, the significantly increased and decreased linkages in adjacent matrices could be obviously found when the brain switched from rest idle to MI task states. Specifically, when the subjects were required to perform lMIs or rMIs, the long-range network linkages that connected the frontal and parietal/occipital lobes decreased during brain reconfiguration process; in contrast, the linkages between bilateral motor areas (i.e., PMc and SMA) were enhanced during MI.

Besides the differences of brain topologies in Figs. 3, 4 further shows the related comparison ($p < 0.05$, FDR correction) of global network and local electrode parameters between rest and task networks. As provided in Fig. 4, the decreased global network properties of lMIs/rMIs deviating
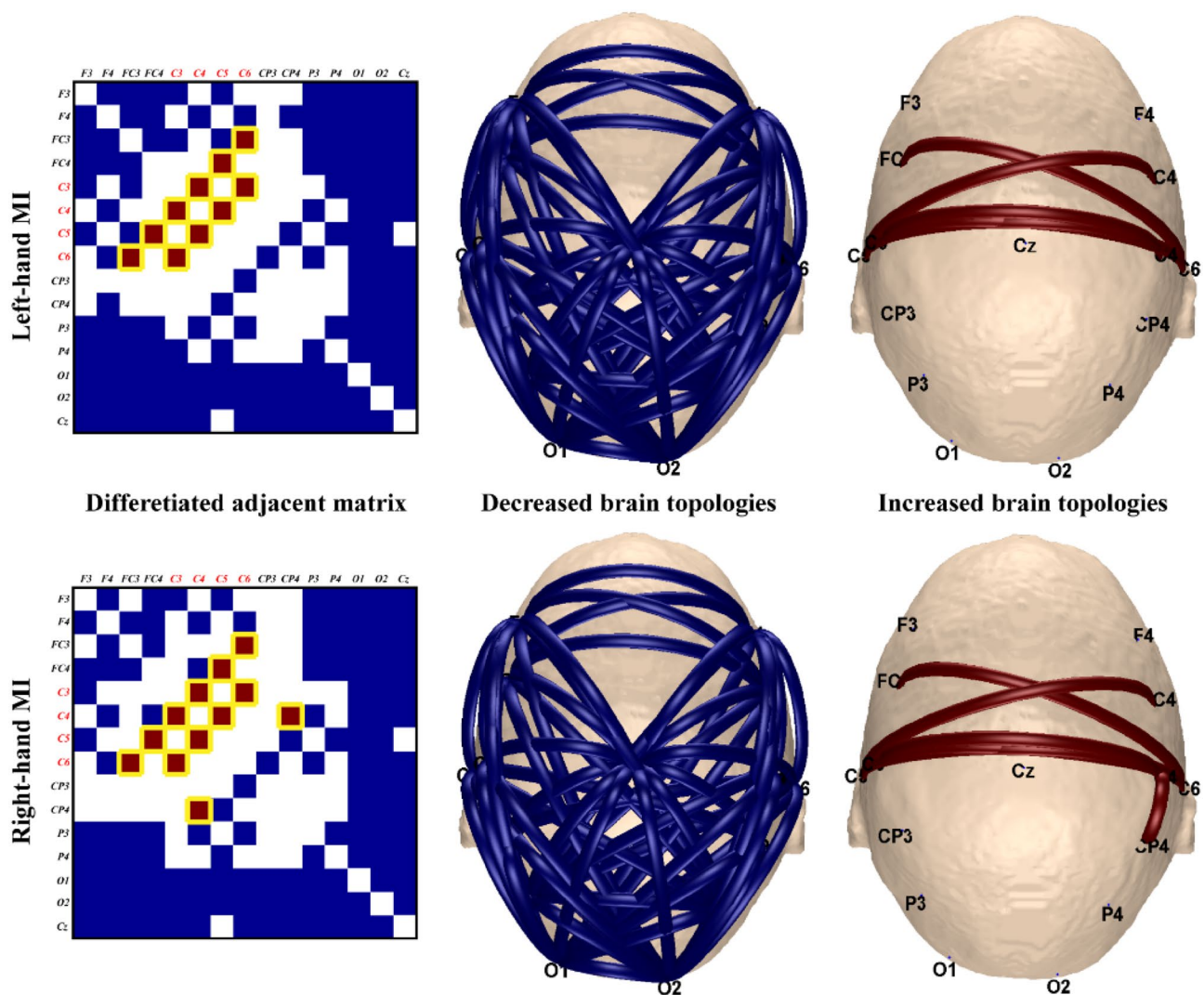
Fig. 3 The reorganized brain network topologies from rest to lMIs/rMIs. The subfigures in first and second row represent the reorganized network topologies of lMIs and rMIs, respectively. The matrices in first column show the reorganized (i.e., increased/decreased) adjacent matrices from rest to task states; the subfigures in second and third column show the corresponding decreased and increased brain network topologies for lMIs/rMIs deviating from rest idle state, respectively

from rest state could be found (Fig. 4a). Specifically, the decreased local clustering coefficients were revealed for both lMIs and rMIs, since some electrodes (i.e., F3, F4, FC3, FC4, P3, P4, O1, O2, and Cz) showed the significantly decreased local network parameters (Fig. 4b), which was similar to the decreased DMN presented in Fig. 3. Unfortunately, although the enhanced motor area related linkages were observed in Fig. 3, the brain topographies in Fig. 4 did not show similar patterns, as no significantly enhanced local clustering coefficients on motor-related electrodes, such as C3, C4, C5, and C6, were observed.

Since the local clustering coefficients showed the similar reconfigured brain pattern with the network topologies, as well as the global network properties, our subsequent analysis would then concentrate on the four properties (i.e., *CC,*

CPL, GE, and *LE*) to uncover the corresponding relationships between concerned parameters (i.e., rest properties vs. task properties and rCNI vs. ERDs). Below Table 1 then gives the relationships of properties between these two types of networks, which reveals that both lMIs and rMIs network are significantly positively correlated ($p < 0.05$, FDR correction) with that of rest network. In other words, the subject who had efficient rest network would have the efficient task network in his/her lMIs or rMIs.

ERD Versus Reconfigured Network

Figure 5 shows the distinct changes of power spectrum on electrodes C3 and C4 for lMIs and rMIs across all subjects, which mainly shows the significant differences of power

Fig. 4 The statistical differences of global network and local electrode parameters between rest idle and task states for lMIs and rMIs. **a** The statistical histograms of global network properties between rest and lMIs/rMIs, and **b** The topographical distributions of reconfigured clustering coefficients on each electrode from rest to task states for lMIs and rMIs. The blue denotes the decreased clustering coefficients with $p < 0.05$, and the white denotes no significant difference between the two brain states
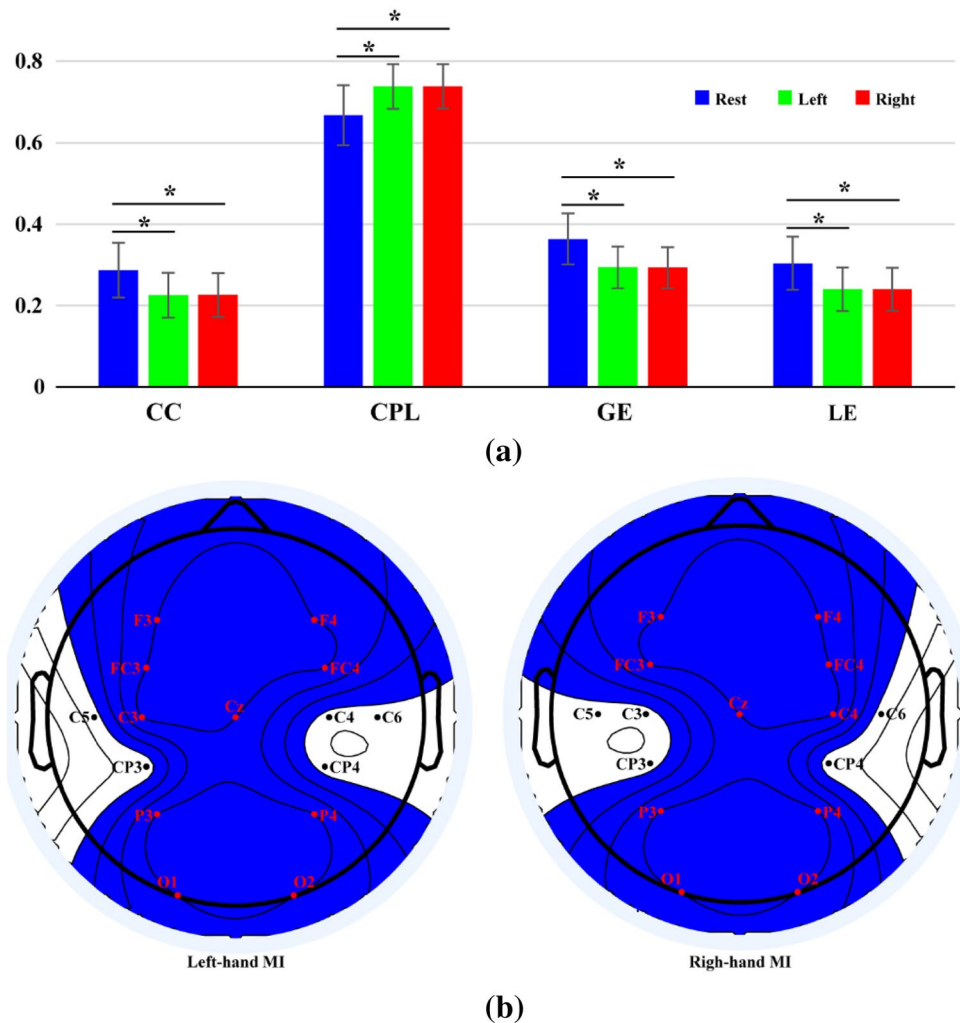

(a)

(b)

Table 1 Correlations of properties between rest and task networks for lMIs and rMIs

	lMIs	rMIs
Clustering coefficient	0.527*	0.524*
Characteristic path length	0.550*	0.547*
Global efficiency	0.581*	0.575*
Local efficiency	0.543*	0.538*

*$P < 0.05$, FDR correction

spectrum at the mu rhythm. Specifically, when the subjects performed the required lMIs, comparing to that on electrode C3, Fig. 5a shows the significantly ($p < 0.05$) decreased power spectrum on electrode C4 at the mu rhythm; in contrast, for the subjects' rMIs, electrode C3 showed the corresponding significantly decreased power spectrum.

When the outlier subjects were removed, Fig. 6 further reveals the relationships (uncorrected) between ERDs and rCNI in both lMIs and rMIs. Specifically, the positive

correlations can be observed between ERD and characteristic path length (lMIs: $r = 0.464$, $p = 0.023$; rMIs: $r = 0.290$, $p = 0.170$), whereas clustering coefficient (lMIs: $r = -0.397$, $p = 0.055$; rMIs: $r = -0.286$, $p = 0.176$), global efficiency (lMIs: $r = -0.466$, $p = 0.022$; rMIs: $r = -0.290$, $p = 0.170$) and local efficiency (lMIs: $r = -0.420$, $p = 0.041$; rMIs: $r = -0.295$, $p = 0.162$) are negatively correlated with ERDs.

Discussion

In our previous study, we probed the efficient brain at rest facilitating the subjects' BCI performance (Zhang et al. 2015), which implied that the efficiently organized brain at rest provides the physiological possibility for the efficient information processing during MI. Other studies also proved the involvements of large-scale brain networks during certain tasks (i.e., MI) (Sharma and Baron 2013; Yan et al. 2013), as well as the functional connectivity updates from rest to task states (Cole et al. 2014; Kaufmann et al.

Fig. 5 The power spectrum on electrodes C3 and C4 for lMIs and rMIs across all subjects. Subfigure (**a**) denotes the power spectrum for required lMIs on electrodes C3 and C4, subfigure (**b**) denotes the power spectrum for required rMIs on electrodes C3 and C4, and black filled rectangles in (**a**) and (**b**) denote the differences of power spectrum between C3 and C4 for lMIs and rMIs under the significance level of 0.05
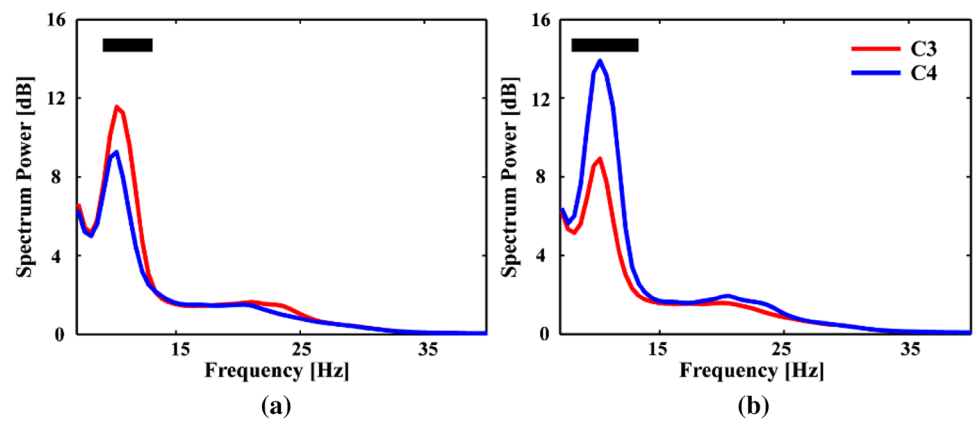
Fig. 6 Pearson correlations between ERD and rCNI in both the lMIs and rMIs. The red filled circles denote the subjects' lMIs, the blue filled circles denote the subjects' rMIs, the grey filled circles denote the excluded subjects' lMIs, and the black filled circles denote the excluded subjects' rMIs. The red and blue solid lines are the regression of ERD to the reconfigured network measurements for the subjects' lMIs and rMIs, respectively
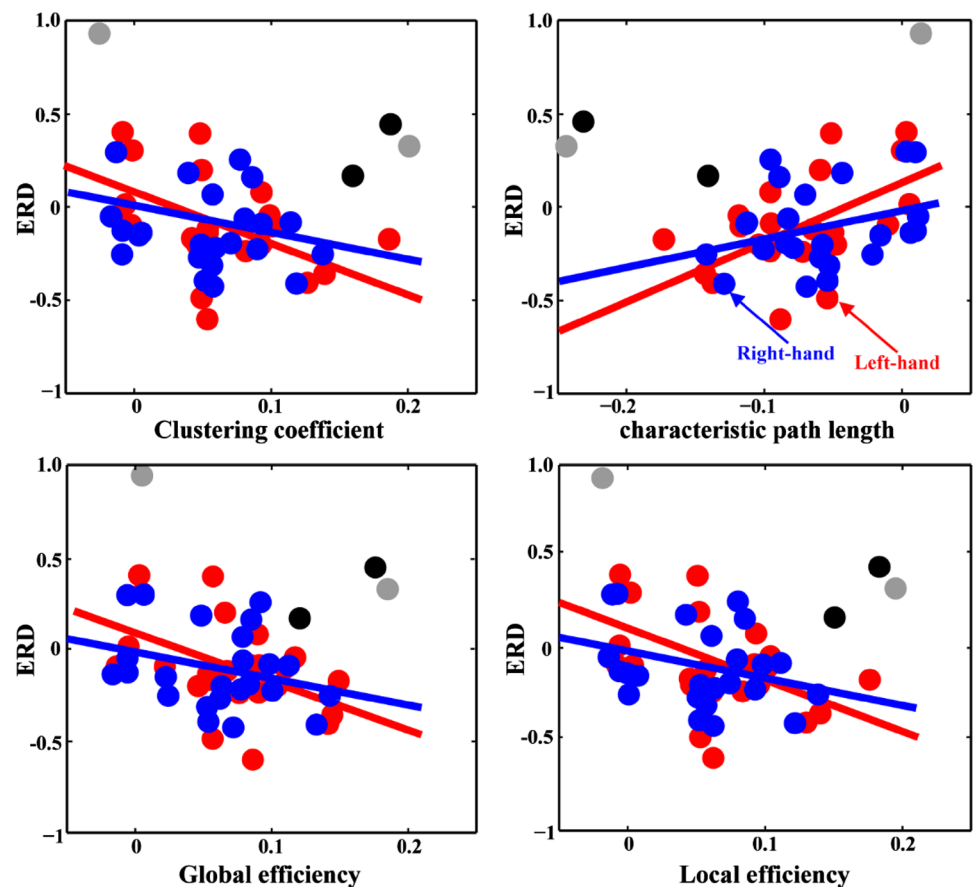
2017; Krienen et al. 2014; Schultz and Cole 2016). Inspired by these findings, in this work, we endeavored to probe the relationships between rest and lMIs/rMIs networks, and to probe the correlations between the degree of brain reconfiguration (i.e., rCNI) and ERDs to decode how our brain reorganizes from rest idle to task states to fulfill the needs of MI information processing.

As brain at rest serves as a fundamental biomarker to infer the information processing during the following tasks, it is interesting to uncover how our brain reorganizes when switching from rest idle to task states, and to probe the relationship between brain reconfiguration and MI. The high correlation coefficients of four properties between two types of networks in Table 1 revealed that the subjects with an efficient brain at rest can evoke the corresponding efficient brain networks during related MI tasks. When referring to the related brain structure, Fig. 3 then shows that when the subjects performed the required lMIs or rMIs, the necessary brain reconfiguration from rest to task states was accompanied, since Fig. 3 revealed the decreased long-range

edges and reconfigured interactions in motor area for both lMIs and rMIs. Moreover, the statistical differences of local electrode parameters (i.e., clustering coefficients) in Fig. 4 further demonstrated the similar trend with the significantly decreased local parameters on electrodes F3, F4, P3, P4, and O1,etc observed. In fact, MI relies on the similar neural structures and processes of motor execution, which involves the contralateral BA4, PMc, parietal areas, and SMA (Sharma and Baron 2013). During MI, multiple brain regions work together in network sense to fulfill the needs during task, which contributes to the subjects' performance (Burianová et al. 2013). In our present study, after 2-min rest, all subjects were instructed to perform the lMIs/rMIs, thereafter, the task-specified brain regions would be activated and accompanied by the necessary brain reorganization (i.e., the resource reconfiguration). As depicted, the desynchronizing process (i.e., ERD) of cortical neurons in the brain will contribute to the subjects' MI performance (Graimann et al. 2002). In our present study, as shown in Figs. 3 and 4, the underlying mechanism might be that the limited brain resources were reconfigured, in which the related linkage strengths of less important long-range edges decreased while the important connections among task-related brain areas (i.e., PMc and SMA) were enhanced to fulfill the needs of the information processing of MI. Moreover, the decreased linkage pattern in Fig. 3 was very close to the default mode network (DMN) of EEG (Chen et al. 2008). Various studies had proved that DMN is negatively correlated with task (Fransson 2006; Singh and Fawcett 2008), i.e., DMN is deactivated in tasks. The decreased topological pattern in current work may also infer the negative correlation of DMN with MI tasks.

Afterwards, Fig. 5 shows that during MI, electrodes C4 and C3 could be obviously observed with the significant power decrease at mu rhythm for lMIs and rMIs, respectively. Being a mental process, MI requires the subjects to mentally imagine the motor behaviors, which leads to the localized power decreases (desynchronizing process) of the rhythmic activity (i.e., mu rhythm) (Pfurtscheller 2001) and further contributes to information processing of MI. In this work, the alerting cues (yellow bars) allowed the subjects to fully prepare for the MIs, and after the bars turned green, the subjects started to perform the imagery of bouncing a ball by his/her left or right hand, which consistently enhanced the neuronal excitability and further led to the power decreases of the mu rhythmic activity during MI.

Since ERD indicates the power bias from the baseline state, we assumed that the rCNI representing the network bias from the resting-state may be physiologically correlated with ERD. The plots in Fig. 6 indeed provided the corresponding evidences that those subjects with smaller ERDs had higher deviated rCNI from rest idle state for both lMIs and rMIs. As illustrated, multiple cognitive brain functions, such as intelligence, are closely related to the efficiency of information processing in the brain, and a more efficient brain network contributes to the better cognition ability (i.e., higher intelligence) (Douw et al. 2011; van den Heuvel et al. 2009; Zhou et al. 2012), as well as the more efficient brain updates (i.e., functional connectivity) from rest idle to task states (Cole et al. 2014; Krienen et al. 2014; Schultz and Cole 2016). The deviated rCNI from rest idle state in Fig. 6, that indexes the efficiency of brain updates from rest idle to MI task states, demonstrated the close relationships (uncorrected) with the desynchronizing process during MI; this further implied that the efficient brain reconfiguration when switching from rest idle to task states can promise the brain at task to reallocate the physiological resources to form the efficient networks for processing the MI related information, which ultimately influenced the BCI performance, i.e., the ERDs in current work. In other words, the more efficient brain reconfiguration is, the more obvious ERD will be (i.e., the more obvious ERD indicates the more bias from the baseline state). Since most of the involved subjects were the right-handedness, when they were required to perform rMIs, the much smaller inter-individual variability of ERDs existed compared to that in lMIs (i.e., the subjects could evoke the relatively stable ERDs for the right MI). At the same time, for the right-handed subjects, the left MI will involve more reconfiguration of networks compared to the right MI (i.e., left MI needs the more brain resources for information processing than right MI). Therefore, the relatively stronger relationships are revealed in Fig. 6 for the left MI. Moreover, due to some other factors like the relatively small subject number, no significant relationships between rCNI and ERDs for rMIs were revealed in current study.

As MI has been regarded as an effective way widely used in the motor function rehabilitation, our proposed index (i.e., rCNI) can thereby be a potential feedback biomarker to establish the rehabilitation system to perform the effectively training for those patients with the deficit of motor function, and is helpful to establish the effective strategy for the training of MI-BCI users. One possible limitation might be that the present study mainly focused on the network reconfiguration at the mu rhythm (8 ~ 13 Hz) band without considering the different network patterns in other EEG frequency bands, which is worthwhile to be probed in future work. Due to the volume conduction on scalp EEG, the performed network analysis in current study may introduce some artificial linkages even if the scalp EEG is sparsely recorded over scalp. Theoretically, the network analysis combined with EEG source localization may be a more meaningful way to alleviate the effect of volume conduction, which will be a promising alternative approach for the reliable network analysis.

Conclusion

In the present study, our findings mainly implied that the subjects with efficient rest networks showed more efficient brain reconfiguration during MI. In other words, the efficient brain reconfiguration from rest idle to task states guaranteed the brain to efficiently process the information of the required MI tasks (i.e., lMIs or rMIs), where the higher degree the network is reconfigured, the more obvious ERDs (larger bias from baseline) will be.

Compliance with Ethical Standards

Conflict of interest The authors declare that they have no conflict of interest.

Ethical Approval All procedures performed in studies involving human participants were in accordance with the ethical standards of Institution Research Ethics Board of the University of Electronic Science and Technology of China, and with the 1964 Helsinki declaration and its later amendments or comparable ethical standards.

Informed Consent Informed consent was obtained from all individual participants included in the study.

References

Blankertz B, Sannelli C, Haider S et al (2010) Neurophysiological predictor of SMR-based BCI performance. NeuroImage 51(4):1303–1309. https://doi.org/10.1016/j.neuroimage.2010.03.022

Bullmore E, Sporns O (2009) Complex brain networks: graph theoretical analysis of structural and functional systems. Nat Rev Neurosci 10(3):186–198. https://doi.org/10.1038/nrn2575

Burianová H, Marstaller L, Sowman P et al (2013) Multimodal functional imaging of motor imagery using a novel paradigm. NeuroImage 71:50–58. https://doi.org/10.1016/j.neuroimage.2013.01.001

Chen AC, Feng W, Zhao H, Yin Y, Wang P (2008) EEG default mode network in the human brain: spectral regional field powers. NeuroImage 41(2):561–574. https://doi.org/10.1016/j.neuroimage.2007.12.064

Cole MW, Bassett DS, Power JD, Braver TS, Petersen SE (2014) Intrinsic and task-evoked network architectures of the human brain. Neuron 83(1):238–251. https://doi.org/10.1016/j.neuron.2014.05.014

Douw L, Schoonheim M, Landi D et al (2011) Cognition is related to resting-state small-world network topology: an magnetoencephalographic study. Neuroscience 175:169–177. https://doi.org/10.1016/j.neuroscience.2010.11.039

Fransson P (2006) How default is the default mode of brain function?: further evidence from intrinsic BOLD signal fluctuations. Neuropsychologia 44(14):2836–2845. https://doi.org/10.1016/j.neuropsychologia.2006.06.017

Friedrich EV, McFarland DJ, Neuper C, Vaughan TM, Brunner P, Wolpaw JR (2009) A scanning protocol for a sensorimotor rhythm-based brain-computer interface. Biol Psychol 80(2):169–175. https://doi.org/10.1016/j.biopsycho.2008.08.004

Friston KJ, Harrison L, Penny W (2003) Dynamic causal modelling. NeuroImage 19(4):1273–1302. https://doi.org/10.1016/S1053-8119(03)00202-7

Graimann B, Huggins J, Levine S, Pfurtscheller G (2002) Visualization of significant ERD/ERS patterns in multichannel EEG and ECoG data. Clin Neurophysiol 113(1):43–47. https://doi.org/10.1016/S1388-2457(01)00697-6

Iturria-Medina Y, Sotero RC, Canales-Rodríguez EJ, Alemán-Gómez Y, Melie-García L (2008) Studying the human brain anatomical network via diffusion-weighted MRI and Graph Theory. NeuroImage 40(3):1064–1076. https://doi.org/10.1016/j.neuroimage.2007.10.060

Kaufmann T, Alnaes D, Brandt CL et al (2017) Task modulations and clinical manifestations in the brain functional connectome in 1615 fMRI datasets. NeuroImage 147:243–252. https://doi.org/10.1016/j.neuroimage.2016.11.073

Krienen FM, Yeo BT, Buckner RL (2014) Reconfigurable task-dependent functional coupling modes cluster around a core functional architecture. Phil Trans R Soc B 369(1653):20130526. https://doi.org/10.1098/Rstb.2013.0526

Li Y, Long J, Yu T, Yu Z, Wang C, Zhang H, Guan C (2010) An EEG-based BCI system for 2-D cursor control by combining Mu/Beta rhythm and P300 potential. IEEE Trans Biomed Eng 57(10):2495–2505. https://doi.org/10.1109/Tbme.2010.2055564

Li Y, Pan J, Wang F, Yu Z (2013) A hybrid BCI system combining P300 and SSVEP and its application to wheelchair control. IEEE Trans Biomed Eng 60(11):3156–3166. https://doi.org/10.1109/Tbme.2013.2270283

Li F, Liu T, Wang F et al (2015) Relationships between the resting-state network and the P3: evidence from a scalp EEG study. Sci Rep 5:15129. https://doi.org/10.1038/Srep15129

Li F, Chen B, Li H et al (2016a) The time-varying networks in P300: a task-evoked EEG study. IEEE Trans Neural Syst Rehab Eng 24(7):725–733. https://doi.org/10.1109/Tnsre.2016.2523678

Li Y, Pan J, Long J, Yu T, Wang F, Yu Z, Wu W (2016b) Multimodal BCIs: target detection, multidimensional control, and awareness evaluation in patients with disorder of consciousness. Proc IEEE 104(2):332–352. https://doi.org/10.1109/Jproc.2015.2469106

Li F, Peng W, Jiang Y et al (2018) The dynamic brain networks of motor imagery: time-varying causality analysis of scalp EEG. Int J Neural Syst:1850016. https://doi.org/10.1142/s0129065718500168

Long J, Li Y, Wang H, Yu T, Pan J, Li F (2012) A hybrid brain computer interface to control the direction and speed of a simulated or real wheelchair. IEEE Trans Neural Syst Rehab Eng 20(5):720–729. https://doi.org/10.1109/Tnsre.2012.2197221

Lotze M, Halsband U (2006) Motor imagery. J Physiol-Paris 99(4):386–395. https://doi.org/10.1016/j.jphysparis.2006.03.012

Miller KJ, Schalk G, Fetz EE, den Nijs M, Ojemann JG, Rao RP (2010) Cortical activity during motor execution, motor imagery, and imagery-based online feedback. Proc Natl Acad Sci USA 107(9):4430–4435. https://doi.org/10.1073/pnas.1002462107

Mulder T (2007) Motor imagery and action observation: cognitive tools for rehabilitation. J Neural Transm 114(10):1265–1278. https://doi.org/10.1007/s00702-007-0763-z

Pfurtscheller G (2001) Functional brain imaging based on ERD/ERS. Vision Res 41(10):1257–1260. https://doi.org/10.1016/S0042-6989(00)00235-2

Pfurtscheller G, Da Silva FL (1999) Event-related EEG/MEG synchronization and desynchronization: basic principles. Clin Neurophysiol 110(11):1842–1857. https://doi.org/10.1016/S1388-2457(99)00141-8

Pfurtscheller G, Neuper C (1997) Motor imagery activates primary sensorimotor area in humans. Neurosci Lett 239(2):65–68. https://doi.org/10.1016/S0304-3940(97)00889-6

Pilgramm S, de Haas B, Helm F, Zentgraf K, Stark R, Munzert J, Krüger B (2016) Motor imagery of hand actions: Decoding the content of motor imagery from brain activity in frontal and parietal motor areas. Hum Brain Mapp 37(1):81–93. https://doi.org/10.1002/hbm.23015

Raichle ME, MacLeod AM, Snyder AZ, Powers WJ, Gusnard DA, Shulman GL (2001) A default mode of brain function. Proc Natl Acad Sci USA 98(2):676–682. https://doi.org/10.1073/pnas.98.2.676

Ramos-Loyo J, Gonzalez-Garrido AA, Amezcua C, Guevara MA (2004) Relationship between resting alpha activity and the ERPs obtained during a highly demanding selective attention task. Int J Psychophysiol 54(3):251–262. https://doi.org/10.1016/j.ijpsycho.2004.05.008

Rubinov M, Sporns O (2010) Complex network measures of brain connectivity: uses and interpretations. NeuroImage 52(3):1059–1069. https://doi.org/10.1016/j.neuroimage.2009.10.003

Sakkalis V (2011) Review of advanced techniques for the estimation of brain connectivity measured with EEG/MEG. Comput Biol Med 41(12):1110–1117. https://doi.org/10.1016/j.compbiomed.2011.06.020

Schultz DH, Cole MW (2016) Higher Intelligence Is Associated with Less Task-Related Brain Network Reconfiguration. J Neurosci 36(33):8551–8561. https://doi.org/10.1523/Jneurosci.0358-16.2016

Sharma N, Baron J-C (2013) Does motor imagery share neural networks with executed movement: a multivariate fMRI analysis. Front Hum Neurosci 7:564. https://doi.org/10.3389/Fnhum.2013.00564

Sharma N, Pomeroy VM, Baron J-C (2006) Motor imagery a backdoor to the motor system after stroke? Stroke 37(7):1941–1952. https://doi.org/10.1161/01.Str.0000226902.43357.Fc

Singh KD, Fawcett I (2008) Transient and linearly graded deactivation of the human default-mode network by a visual detection task. NeuroImage 41(1):100–112. https://doi.org/10.1016/j.neuroimage.2008.01.051

Sporns O, Tononi G, Edelman GM (2000) Connectivity and complexity: the relationship between neuroanatomy and brain dynamics. Neural Networks 13(8):909–922. https://doi.org/10.1016/S0893-6080(00)00053-8

Stam CV, Van Straaten E (2012) The organization of physiological brain networks. Clin Neurophysiol 123(6):1067–1087. https://doi.org/10.1016/j.clinph.2012.01.011

Toppi J, Petti M, Mattia D, Babiloni F, Astolfi L (2015) Time-varying effective connectivity for investigating the neurophysiological basis of cognitive processes. In: Sakkalis V (ed) Modern electroencephalographic assessment techniques: theory and applications. Springer New York, New York, pp 171–204. https://doi.org/10.1007/7657_2014_69

van den Heuvel MP, Hulshoff Pol HE (2010) Exploring the brain network: a review on resting-state fMRI functional connectivity. Eur Neuropsychopharmacol 20(8):519–534. https://doi.org/10.1016/j.euroneuro.2010.03.008

van den Heuvel MP, Stam CJ, Kahn RS, Pol HEH (2009) Efficiency of functional brain networks and intellectual performance. J Neurosci 29(23):7619–7624. https://doi.org/10.1523/Jneurosci.1443-09.2009

Xu P, Xiong X, Xue Q et al (2014a) Differentiating between psychogenic nonepileptic seizures and epilepsy based on common spatial pattern of weighted EEG resting networks. IEEE Trans Biomed Eng 61(6):1747–1755. https://doi.org/10.1109/TBME.2014.2305159

Xu P, Xiong X, Xue Q et al (2014b) Recognizing mild cognitive impairment based on network connectivity analysis of resting EEG with zero reference. Physiol Meas 35(7):1279–1298. https://doi.org/10.1088/0967-3334/35/7/1279

Yan J, Sun J, Guo X, Jin Z, Li Y, Li Z, Tong S (2013) Motor imagery cognitive network after left ischemic stroke: study of the patients during mental rotation task. PLoS ONE 8(10):e77325. https://doi.org/10.1371/journal.pone.0077325

Yao Z, Zhang Y, Lin L, Zhou Y, Xu C, Jiang T, Initiative AsDN (2010) Abnormal cortical networks in mild cognitive impairment and Alzheimer's disease. PLoS Comput Biol 6(11):e1001006. https://doi.org/10.1371/journal.pcbi.1001006

Yu T, Li Y, Long J, Gu Z (2012) Surfing the internet with a BCI mouse. J Neural Eng 9(3):036012. https://doi.org/10.1088/1741-2560/9/3/036012

Zhang Z, Liao W, Chen H et al (2011) Altered functional-structural coupling of large-scale brain networks in idiopathic generalized epilepsy. Brain 134(10):2912–2928. https://doi.org/10.1093/brain/awr223

Zhang R, Yao D, Valdés-Sosa PA et al (2015) Efficient resting-state EEG network facilitates motor imagery performance. J Neural Eng 12(6):066024. https://doi.org/10.1088/1741-2560/12/6/066024

Zhang T, Liu T, Li F et al (2016) Structural and functional correlates of motor imagery BCI performance: Insights from the patterns of fronto-parietal attention network. NeuroImage 134:475–485. https://doi.org/10.1016/j.neuroimage.2016.04.030

Zhou G, Liu P, He J et al (2012) Interindividual reaction time variability is related to resting-state network topology: an electroencephalogram study. Neuroscience 202:276–282. https://doi.org/10.1016/j.neuroscience.2011.11.048